

Search for potential Compressed Air Energy Storage sites in Switzerland

Conference Paper**Author(s):**

Pimentel, Erich; Brauchart, Alice; [Anagnostou, Georgios](#) 

Publication date:

2023-04-12

Permanent link:

<https://doi.org/10.3929/ethz-b-000614350>

Rights / license:

[Creative Commons Attribution-NonCommercial-NoDerivatives 4.0 International](#)

Originally published in:

<https://doi.org/10.1201/9781003348030-22>

Search for potential compressed air energy storage sites in Switzerland

E. Pimentel & G. Anagnostou
ETH Zurich, Zurich, Switzerland

A. Brauchart
ETH Zurich, Zurich, Switzerland
(currently: *Rothpletz, Lienhard + Cie AG, Zurich, Switzerland*)

ABSTRACT: The energy transition process in Switzerland foresees a move away from nuclear energy. This calls for an expansion of alternative energy sources such as solar or wind. Since these types of energy generation depend on the weather, the energy generated must be stored to be available on demand. In addition to pumped storage plants, compressed air energy storage (CAES) in underground cavities offers a potential solution for this problem. The economic viability of a CAES system depends on the investment costs as well as the overall efficiency of the system, *i.e.*, storage and recovery of the energy. The paper describes the search for a suitable site in Switzerland for an envisioned adiabatic, high pressure (100 bar) CAES with the potential to store 500 MWh of energy. First, the minimum dimensions and possible arrangements of all the cavities required by the CAES facility are determined. Subsequently, relevant hazard scenarios are identified and analysed from the geotechnical viewpoint. A determination is then made of the requirements, such as rock strength, overburden or distance to the valley flanks of the high-pressure underground chamber. In addition, potential damage to the chamber's sealing is analysed and the plug of the high-pressure chamber is dimensioned structurally. Finally, potential sites are selected with the help of a GIS system incorporating the geological and topographical map of Switzerland.

1 INTRODUCTION

Within the scope of a research project of the Swiss Federal Office of Energy (Amberg *et al.* 2020) we analysed the selection criteria and investigated the availability of suitable potential sites for an underground facility for storing energy in the form of compressed air ("Compressed Air Energy Storage" or CAES) with a storage potential of 500 MWh. CAES systems are used for the short-term storage of surplus energy from wind or solar power plants. The energy is stored in the form of highly pressurised air and, when needed, it can be recovered by releasing the air into turbines connected to a generator which feeds into the energy grid.

The paper starts with a brief description of the various CAES concepts and systems (Section 2) and continues with a discussion of geometric aspects of CAES systems (Section 3). Subsequently, the most important geotechnical-structural hazards are discussed, that is (Perazzelli and Anagnostou 2016): failure and loss of tightness of the cavity sealing (Section 4); uplift or lateral failure of the rock between cavity and surface (Section 5); and failure or loss of serviceability of the plug closing the pressurised cavern (Section 6). Finally, zones are selected for the location of potential sites for a CAES-plant using a GIS system and taking the various criteria into account (Section 7).

To avoid high investment costs for underground construction, only sites with very good geological conditions (fault-free rock mass, only sporadic and closed discontinuities) are considered and, consistently with this overarching planning prerequisite, the assessments of Sections 4–6 are based upon the parameters of very high-quality rocks.

2 CAES CONCEPTS AND SYSTEMS

Large air losses over decades are decisive for the economic efficiency of a CAES plant. In addition, the loss of tightness may impair overall stability, as it will result in the development of high air pressures within the overlying rock mass, thus increasing uplift risk (Perazzelli and Anagnostou 2016). In order to limit loss of air during pressurisation, a sealing must be installed even in good rock conditions. The chamber walls can be lined with a composite system consisting of a supporting and levelling reinforced shotcrete layer, a synthetic protective layer and a sealing membrane (Figure 1). Details about the requirements for the membrane and the investigations performed into the suitability of commercially available products can be found in Amberg *et al.* (2020).

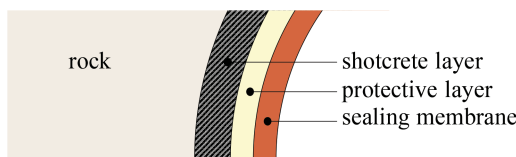


Figure 1. Composite lining system of the pressurised chamber (not to scale).

When compressing air, heat is produced, whereby, according to the thermal equation for ideal gases, the air temperature increases linearly with the pressure. In the cavities, very high gas temperatures and extreme temperature changes must be avoided as they pose a risk to the sealing membrane. There are two possible CAES concepts (Roos, 2021): the diabatic CAES and the advanced adiabatic CAES (AA-CAES).

In a diabatic CAES plant, the heat generated during pressurisation of the cavity is released to atmosphere and additional heat is introduced before compressed air enters the turbine during discharging. In an AA-CAES plant, the heat is captured in thermal-energy storage elements (TES) during charging and the air is re-heated with this thermal energy during discharging. This leads to a higher overall efficiency of the system. The present investigation focuses on AA-CAES plants. For practical reasons the TES elements are placed inside the pressurised chamber and they are therefore decisive for the minimum chamber cross section. Innovative TES are described in Zanganeh *et al.* (2012) and Roos (2021).

For reasons of efficiency, the air compression and air expansion take place in two pressure stages and therefore a low-pressure and a high-pressure chamber with TES (LPCh and HPCh, respectively) and turbines are needed (Amberg *et al.*, 2020). The CAES plant must additionally contain machine and control rooms as well as access galleries and air charging/discharging adits.

3 PRESSURISED CHAMBER LAYOUT

The HPCh is the geotechnically most demanding structure among the underground openings required for a CAES plant. In the present case, the required volume for air storage is 177000 m³ and the nominal pressure equals 100 bar (Amberg *et al.*, 2020). The nominal pressure in the LPCh is considerably lower (10 bar). Thus, the design is less demanding for the LPCh and the other (non-pressurised) underground structures. In the following, only aspects associated with the HPCh will be discussed.

Air losses are unavoidable due to diffusion of air molecules through the membrane. The losses are proportional to the surface area exposed to compressed air. Spherical chambers offer the advantage of the smallest area relative to their volume, but they must be discarded because of excavation difficulties and cost. For a given storage volume, the surface area of a cylinder decreases with increasing diameter. Therefore, larger diameter chambers are more efficient for CAES operation.

The TES are important for the geometry of the HPCh on account of their large dimensions and total volume. In the present case, four TES are needed. They can be placed either one on top of the other or one behind the other. The vertical arrangement would necessitate a 30 m diameter shaft. Due to additional required air storage volume, the height of the shaft for the HPCh would be 275 m (Figure 2a). In the case of horizontal arrangement, a chamber approximately 260 m long with a diameter of 31 m would be needed (Figure 2b), but a combination of a shorter and larger-diameter chamber with a longer and smaller-diameter chamber is also possible (Figure 2c); the latter may be favourable from the construction viewpoint.

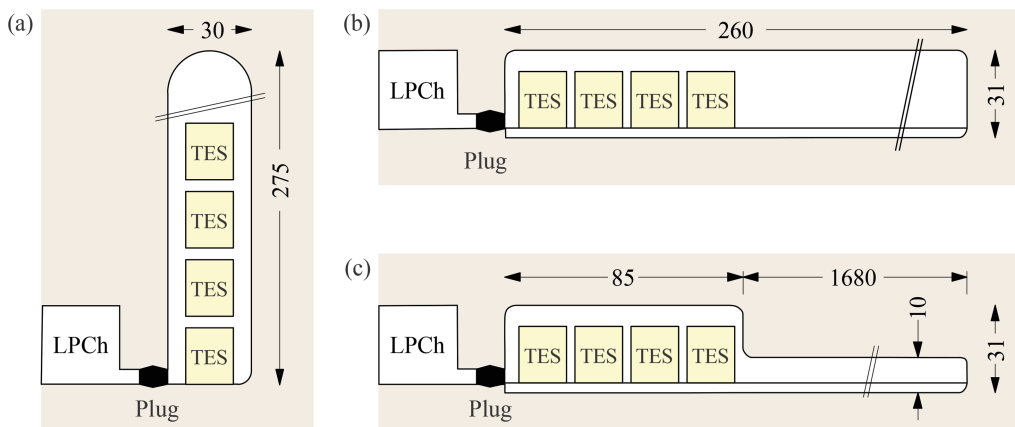


Figure 2. Possible layouts of the high-pressure chambers.

4 ROCK CRACKING AND DAMAGE TO THE COMPOSITE LINING SYSTEM

4.1 Rock discontinuities

Depending on air pressure and secondary rock stresses (the stresses prevailing after excavation but before pressurisation), existing rock discontinuities may open or new cracks may develop during pressurisation. Discontinuities can open only if the pressurisation leads to tensile tangential stresses at the periphery of the chamber.

There are knowledge gaps about rock mass behaviour during cyclic loading with pressurised and depressurised air that causes an alternating opening and closing of rock discontinuities (Perazzelli and Anagnostou, 2016). However, the opening of rock cracks can be excluded and the uncertainty that is associated with the rock mass behaviour can be eliminated, if the secondary (compressive) tangential rock stress is high enough to avoid tensile tangential stresses at 100 bar air pressure in the HPCh. This is the case when the overburden is greater than a critical value H_{min} .

At the same time, limiting the overburden H_{max} to ensure that the rock will behave elastically is better to avoid rock overstressing. Otherwise, a heavier support would be necessary to ensure cavity stability, which could significantly increase the construction costs.

In the following, the determination of H_{min} and H_{max} will be outlined (for details see Amberg *et al.* 2020). Due to the considerable height of the HPCh (shaft: 275 m; cavern: 31 m) and the high air pressure, various situations must be considered:

For determining H_{min} , the location of the smallest secondary rock stresses, that is the top of the chamber, must be considered. The condition to be satisfied (in order to avoid new cracking) is that the tangential rock stress at the chamber crown remains compressive even at the highest operational air pressure of 100 bar.

For determining H_{max} , it is the location of the highest stresses, that is the bottom of the chamber, which is relevant. The condition to be satisfied is that the tangential rock stress under atmospheric pressure must be less than the uniaxial rock mass strength UCS, as the rock lacks the support offered by the compressed air during construction and maintenance.

H_{min} and H_{max} denote thus the minimum depth of the chamber crown and the maximum depth of the chamber invert, respectively. The aforementioned two conditions can be satisfied only if the height of the HPCh is less than the difference between H_{max} and H_{min} . It should be borne in mind that the construction of a CAES in a location that does not fulfil this condition is not necessarily unsuitable, but further investigations would be needed to determine technical and economic viability.

H_{min} and H_{max} can be quantified by means of stress analyses taking account of the *in situ* stresses as well as, for H_{min} , the maximum air pressure. The simplified model of a cylindrical cavity in an elastic medium is considered here and the tangential rock stresses in the cross-sectional plane of the cavity are determined using Kirsch's solution. (The out-of-plane tangential stress is usually less than the tangential stress in the cross-sectional plane and, therefore, does not play a role for H_{max} .) Further assumptions are: the vertical *in situ* stress σ_v represents a principal stress and is equal to the geostatic pressure ($\sigma_v = \gamma H$, where the unit weight γ of the rock is taken equal to 25 kN/m³); the cavern axis coincides with one principal stress axis; the *in situ* horizontal principal stresses σ_{hmin} and σ_{hmax} are equal to $K_{0min} \sigma_v$ and $K_{0max} \sigma_v$, respectively, and the lateral pressure coefficients K_{0min} and K_{0max} depend on the tectonic and topographic conditions (e.g. proximity to a valley).

Table 1. Principal stresses considered in the analysis, calculated maximum depth of chamber invert (H_{max}) and calculated minimum depth of chamber crown (H_{min}).

		$K_{0min} = 1, K_{0max} = 1.7^{(a)}$		$K_{0min} = 0.7, K_{0max} = 1.3^{(b)}$		
High Pressure Chamber	σ_1	σ_3	H_{max} [m]	H_{min} [m]	H_{max} [m]	H_{min} [m]
Shaft, \varnothing 30 m, 275 m high	σ_{hmax}	σ_{hmin}	976	308	1250	500
Cavern, \varnothing 31 m, // σ_{hmax}	σ_v	σ_{hmin}	2000	200	1739	364
Cavern, \varnothing 31 m, // σ_{hmin}	σ_{hmax}	σ_v	976	308	1379	235

(a) Based upon stress measurements of Krietsch *et al.* (2017)

(b) Less pronounced tectonic overprint than indicated by Krietsch *et al.* (2017)

Only few data are available on *situ* stresses. Measurements by Krietsch *et al.* (2017) in the Grimsel massif in Switzerland, a candidate geological formation for CAES sites, indicate lateral pressure coefficients of $K_{0max} = 1.7$ and $K_{0min} = 1.0$, but it is uncertain whether these high values hold for the entire Grimsel massif and other potential sites. For this reason, a case with lower horizontal stresses ($K_{0max} = 1.3$, $K_{0min} = 0.7$), holding for a less pronounced tectonic overprint, is also included in the calculations.

Columns 2 and 3 of Table 1 summarize the principal *in situ* stresses to be included, depending on chamber type, orientation and lateral pressure coefficients, while the 4 last columns show the depths determined for the two sets of lateral pressure coefficients mentioned and the maximum operational pressure of 100 bar (important for H_{min}). An excellent quality rock of UCS = 100 MPa (important for H_{max}) is taken into account. In all the cases investigated, the difference between H_{max} and H_{min} is greater than the chamber height and thus both a shaft and a cavern would in principle be feasible from the viewpoint of rock stressing and cracking. The necessary minimum depth of cover above the chamber crown (H_{min}) depends considerably on the horizontal stresses. This emphasizes the importance of a more detailed knowledge of the *in situ* stresses at the HPCh location.

The H_{max} -values of Table 1 hold for a very high rock UCS (100 MPa). In the case of lower quality rock, the permissible depth would be smaller (H_{max} decreases linearly with the UCS), but this would not play a role as long as H_{max} is greater than the sum of H_{min} and HPCh height. For this limiting case ($H_{max} = H_{min} + \text{HPCh height}$) and the greatest H_{min} listed in Table 1, the required minimum UCS for the shaft and cavern variants is equal to 62 MPa and 23 MPa, respectively. This means that in less favourable geological conditions, the cavern variant would be better than the shaft variant as the required minimum overburden H_{min} is smaller and the required rock quality is lower.

4.2 Damages to the composite lining system

The rock mass around the chamber can sustain a high air pressure without cracking because it is pre-stressed by the secondary (compressive) tangential stresses (Section 4.1). Unlike to the rock, the composite lining is practically stress-free initially, when the air pressure is still atmospheric. Therefore, chamber pressurization inevitably results in tensioning of all components of the composite lining system (Figure 1) and the lining can be damaged by the cyclic loading experienced during the operation of the CAES plant even if the rock behaves elastically and existing cracks remain closed during pressurisation. The following damage types can occur: (a) cracking of the shotcrete layer; (b) tensile failure of the reinforcement of the shotcrete layer; (c) shearing of the sealing membrane; (d) overstretching of the sealing membrane or the protective layer.

- (a) As the stiffnesses of the protective layer and of the sealing membrane are negligible, the tensile stresses developing in the shotcrete layer due to air pressurization increase with the ratio of the shotcrete modulus E_{SC} to the rock modulus E , and will quickly exceed the tensile strength of shotcrete, even if the shotcrete layer is soft relatively to the rock mass. (For example, for a rock modulus E of 40 GPa, a shotcrete modulus E_{sc} of 15 GPa and an air pressure of 100 bar, the tensile stress reaches about 4.5 MPa.) Consequently, cracking of the shotcrete layer can hardly be avoided. The depth of the cracks in the shotcrete layer is limited to its thickness. A favourable crack distribution (characterized by several narrow instead of a few widely open cracks) can be achieved with reinforcement of the shotcrete (possibly fibres).
- (b) The strain experienced by the steel reinforcements (and all other components of the composite lining system) during cavity expansion is equal to the tangential strain of the rock at the cavity wall. If the tangential strain was higher than the yield strain of the steel, then partially irreversible steel strains would develop during the cavity pressurization and expansion phase. Consequently, in the subsequent depressurization phase the steel bars would experience compression and could buckle towards the cavity (*cf.* Perazzelli and Anagnostou 2016), causing bulging of the protective layer and of the sealing membrane. This type of damage can be excluded in the case of a competent rock; for example, if the rock exhibits an elasticity modulus of 20 GPa, the circumferential strain developing at an air pressure of 100 bar would be about 0.065% according to elasticity theory (Kirsch solution, neglecting the lining stiffness), which is clearly less than the yield strain of steel (about 0.2%). Steel fatigue is another potential hazard that should be investigated, but this hazard, too, appears to be relevant rather for lower quality (lower stiffness) rocks (see Perazzelli and Anagnostou 2016). The behaviour of fibre reinforcements has not been investigated within this research project.
- (c) Compressed air may squeeze the protective layer including the membrane into small cracks in the shotcrete and the membrane may fail due to shearing. The membrane may also be damaged in the air pressure release phase due to jamming by a partially closing crack. By ensuring a limited crack width and a sufficiently thick protective layer this damage seems unlikely. However, further investigations into this topic are necessary.
- (d) Due to local rock heterogeneities, irregularities of the rock surface and imperfections in the shotcrete layer, the strain distribution along the chamber circumference will most likely be non-uniform. Therefore, the ultimate strain of the sealing membrane and the

protective layer must be a multiple of the mean tangential strain of the rock to ensure its structural integrity. The products suggested in Amberg *et al.* (2020) fulfil this condition.

5 SAFETY AGAINST UPLIFT OR LATERAL FAILURE

Chamber pressurization may cause uplift of the rock mass up to the surface or, if the chamber is located close to valley flanks, failure of the rock in the horizontal direction, between sidewall and valley. The safety against these failures can be increased by increasing the depth of the chamber and its distance to the valley flanks. As analysed by Perazzelli and Anagnostou (2016), safety with respect to uplift failure of the rock mass is often less critical than the limitation of rock mass deformation and cracking. This is also true in the present case, as we will see subsequently, based upon the extremely conservative assumptions of zero rock cohesion, UCS and tensile strength. The effect of these parameters could be assessed by the series of methods presented or reviewed by Perazzelli and Anagnostou (2018), but such a detailed analysis is not necessary in the present case.

The safety factor, defined as the ratio of resistance to action, is estimated here based upon the limit equilibrium of the simplified failure mechanisms of Figures 3a–3d. The action results from the air pressure acting upon the failure body, while the resistance is taken equal to the weight of the failure body (Figures 3a and 3c) or to the frictional force acting parallel to the horizontal sliding surface (Figures 3b and 3b). The contributions of cohesion and of tensile strength to the resistance are disregarded.

The diagram on the left-hand side of Figure 3 shows the safety factor against uplift as a function of the depth of the HPCh crown. For the depth that is anyway necessary in order to avoid cracking, that is 364 m and 500 m for the cavern and the shaft (Table 1), respectively, the safety factor against uplift equals to about 5 and 2, respectively, which is easily sufficient given the extremely conservative assumptions here.

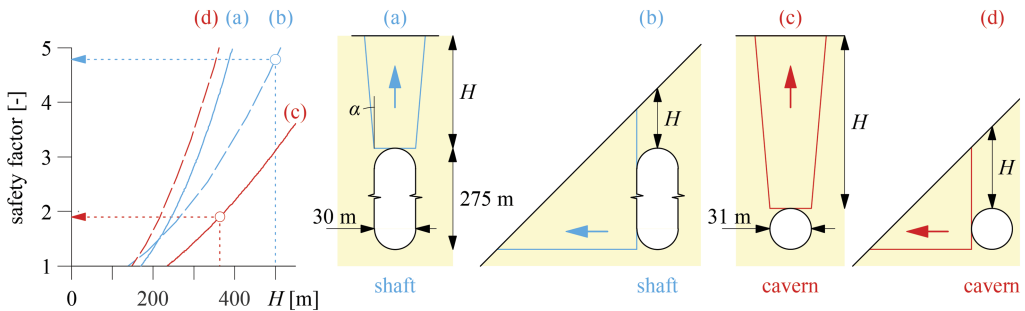


Figure 3. Safety factor against uplift (a, c) or lateral failure (b, d) over depth H of the HPCh crown (mechanisms (a) and (c): assumed angle $\alpha =$ dilatancy angle $=5^\circ$; mechanisms (b) and (d): assumed friction angle $= 35^\circ$).

6 CONCRETE PLUG

Figure 4 shows a concrete plug (schematically, without the penetrations for pipes or access gate), its loading p by the compressed air and the load transfer to the rock (contact pressure σ_N , Figure 4a) and three hazard scenarios: (i) shear failure of the concrete (Figure 4a); (ii) separation of the concrete plug from the rock (Figure 4b); and, (iii), rock failure in the abutment zone under the action of the contact pressure σ_N (Figure 4c).

The first hazard scenario, shear failure of the concrete, is in general the decisive one for determining plug length (Perazzelli and Anagnostou 2016). For a concrete shear strength of 1.5 MPa, air pressure of 100 bar and a \varnothing 7.5 m access gallery, the necessary plug length L_p is equal to 12.5 m.

Hazard scenario (ii), the concrete-rock separation, is critical for serviceability and stability (Okuno *et al.*, 2009). Opening of the concrete-rock joint is inevitable and can be quantified by numerical stress analyses. It necessitates a special structural detailing of the composite lining, so that the latter can bridge the gap.

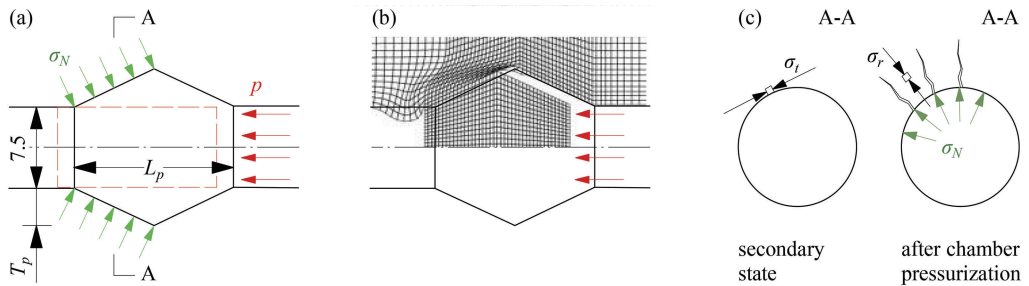


Figure 4. Hazard scenarios for the concrete plug: (a) shear failure of concrete along horizontal dashed lines; (b) concrete-rock separation (numerical results after Perazzelli and Anagnostou, 2016); (c) rock cracking and crushing.

The aforementioned stress analyses are also valuable for evaluating hazard scenario (iii), the stability of the rock abutments. Rock overstressing is not critical for plug design even in the case of moderate strength rocks (Perazzelli and Anagnostou, 2016). This hazard scenario is discussed here based upon a simple model in order to illustrate the nature of rock loading and failure at the plug abutments. The cavity in the area of the plug experiences an expansion under the action of the pressure σ_N . This results in a decrease in the tangential stress (σ_t in Figure 4c, l.h.s.) in the rock around the plug. If the *in situ* stresses are not sufficiently high, then σ_t will decrease to zero, become afterwards negative (tensile) and reach the tensile strength of the rock. The latter will fail in tension and, consequently, radial cracks will develop (Figure 4c, r.h.s.). Then the rock will be loaded uniaxially (experiencing only the radial stress σ_r) by the abutment pressure σ_N and, if σ_N exceeds the UCS of the rock, it will be crushed. Both the tangential rock failure in tension and the radial rock failure in uniaxial compression can be avoided by limiting the abutment stress σ_N needed for plug equilibrium. This can be achieved by foreseeing a sufficient plug conicity (T_p in Figure 4a). The average contact stress σ_N can be calculated analogously to the joint pressure in a taper press connection (conservatively neglecting the friction between concrete and rock), while the expansion-induced tangential rock stresses can be estimated analogously to Section 4.1. In the present case, the conicity $T_p = 0.9$ m for the shaft and 1.5 m for the cavern. The difference in conicity is due to the different secondary rock stresses; the latter are higher (more favourable concerning cracking) in the deeper-located invert of the shaft.

7 POTENTIAL SITES FOR A CAES-PLANT

The economic viability of a CAES-plant depends heavily on the location. Therefore, only those sites are considered that are likely to be cost-effective, *inter alia* with regard to the geological-geotechnical conditions. The set of potential sites is narrowed down stepwise using a geographic information system (GIS).

Firstly, using the geological map of Switzerland, areas with rock of expectedly good quality near the surface are pre-selected. Specifically, only areas with igneous rocks (or metamorphic rocks of igneous origin) are considered (Figure 5a).

For network efficiency and connection cost reasons, the distance of the CAES plant to existing high-voltage grid lines should not exceed 10 km. Consequently, a series of 20 km wide corridors along all high-voltage lines are considered in the second layer (Figure 5b).

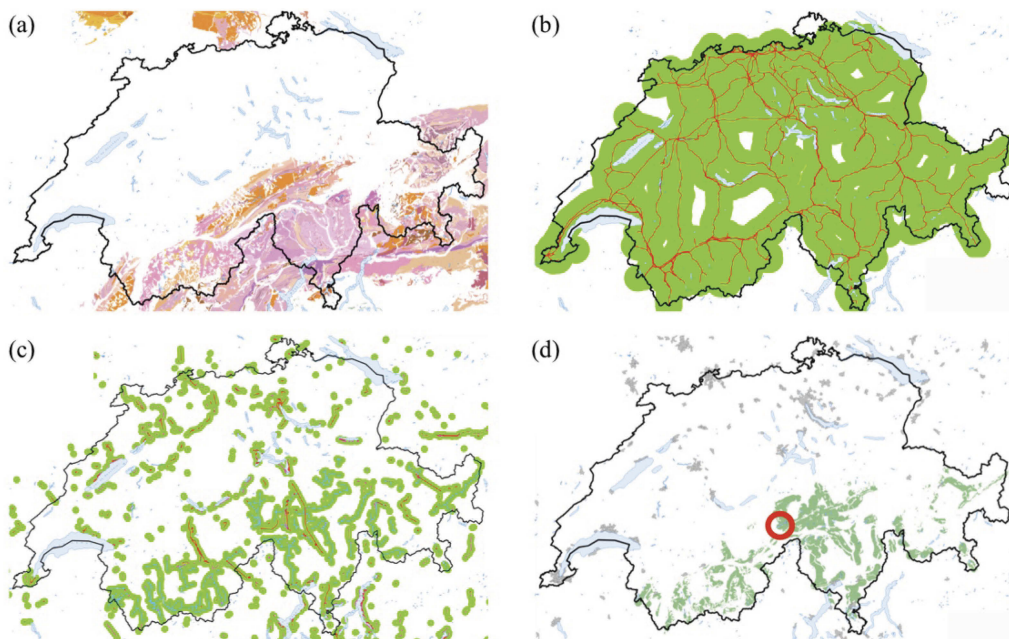


Figure 5. Selection of potential sites for a CAES-plant in Switzerland: (a) favourable geology; (b) vicinity of high-voltage lines; (c) availability of geological-geotechnical data; (d) synthesis (red circle: region of the Figure 6 examples).

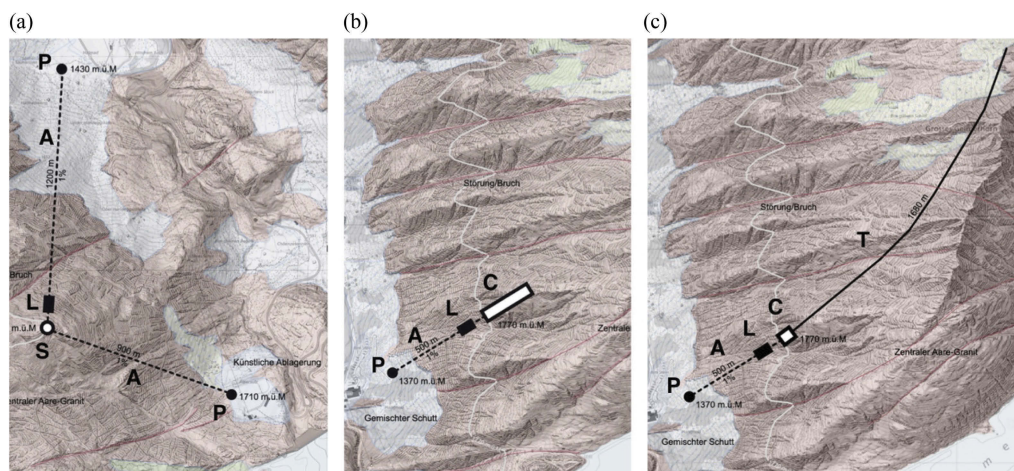


Figure 6. Examples of suitable sites. (a) shaft; (b) cavern; (c) cavern-tunnel combination (P = portal; A = access tunnel; L = LPCh or control cavity; S = HPCh (shaft); C = HPCh (cavern); T = HPCh (tunnel)).

The geological-geotechnical data and experience from the planning and construction stages of existing hydropower plants and traffic tunnels can be used to significantly increase the reliability of the rock mass assessment at this early stage of the project. Therefore, a 5 km wide corridor along/around existing underground structures was considered in the third layer (Figure 5c).

The zones marked in green in Figure 5d satisfy all these criteria and they are additionally not close to urban areas, so they served as a starting point for the next step, which was the higher resolution search at a scale 1:10000 and the identification of specific sites. Among other

aspects, such as site accessibility via existing infrastructure, sites close to steep slopes are preferable in order to reach the required minimum overburden with an access tunnel that is as short as possible, while sites with portals in loose rock or soft ground (especially talus debris cones) are avoided (see Amberg *et al.* 2020 for details). Figure 6 shows examples of suitable CAES sites in the Grimsel region (marked by a red circle in Figure 5d).

8 CONCLUSIONS

A systematic procedure has been presented for selecting suitable and cost-efficient potential sites for a CAES-plant with an energy storing capacity of 500 MWh. The procedure analyses the most relevant hazard scenarios and can be easily adopted to other plants with different storage capacities or pressures. For sites with less favourable geological conditions, the hazard scenarios will be similar, although there may be a need for further investigations and more refined numerical models and assessment methods to prove the safety and serviceability of the system.

REFERENCES

- Amberg, F., Anagnostou, G., Boissonnas, Y., Brauchart, A., Haselbacher, A., Londschein, M., Pimentel, E., & Zanganeh, G. (2020). AASD – Sealing and Design of Underground Caverns for Compressed Air Storage Plants (in German). BFE Bundesamt für Energie. Project Nr. SI/501932. (url: <https://www.aramis.admin.ch/Default?DocumentID=66638&Load=true>).
- Krietsch, H., Gischig, V., Jalali, M., Amann, F., Evans, K., Doetsch, J., & Valley, B. (2017). Stress measurements in crystalline rock: Comparison of overcoring, hydraulic fracturing and induced seismicity results. In 51st US Rock Mechanics/Geomechanics Symposium, San Francisco, USA.
- Okuno, T., Wakabayashi, N., Niimi, K., Kurihara, Y., & Iwano, M. (2009). Advanced natural gas storage system and verification tests of lined rock cavern - ANGAS project in Japan. *International Journal of the JCRM*, 5(2):95–102.
- Perazzelli, P. & Anagnostou, G. (2016). Design issues for compressed air energy storage in sealed underground cavities. *J Rock Mech Geotech Eng*, 8: 314–328.
- Perazzelli, P., & Anagnostou, G. (2018). Upper bound limit analysis of uplift failure in pressurized sealed rock tunnels. *Int J Numer Anal Methods Geomech*, 42:719–735.
- Roos, Ph. (2021). Sensible thermal-energy storage for adiabatic compressed air energy storage plants: Design and optimization. PhD Thesis, ETH Zurich No. 27169 (url: doi: 10.3929/ethz-b-000491538)
- Zanganeh, G., Pedretti, A., Zavattoni, S., Barbato, M. & Steinflod, A. (2012). Packed-bed thermal storage for concentrated solar power – Pilot-scale demonstration and industrial-scale design. *Solar Energy*